

Supporting Information to the research article:

Microphysics of inelastic deformation in reservoir sandstones from the
seismogenic center of the Groningen gas field

R.P.J. Pijenburg and C.J. Spiers

Journal of the Mechanics and Physics of Solids

Content:

Figures S1 and S2

Introduction:

This file contains two pieces of supporting information. In Figure S1, we illustrate the porosity versus normal stress data implied by the void ratio versus normal stress data reported by [Brown *et al.*, 2017], plus the data treatment employed to obtain the clay consolidation behavior described by Equation 7 of the main text. In Figure S2 we provide additional geometrical insights for the estimation of the strain increment due to multi-edge cracking, as described in Section 7.5.2 of the main text.

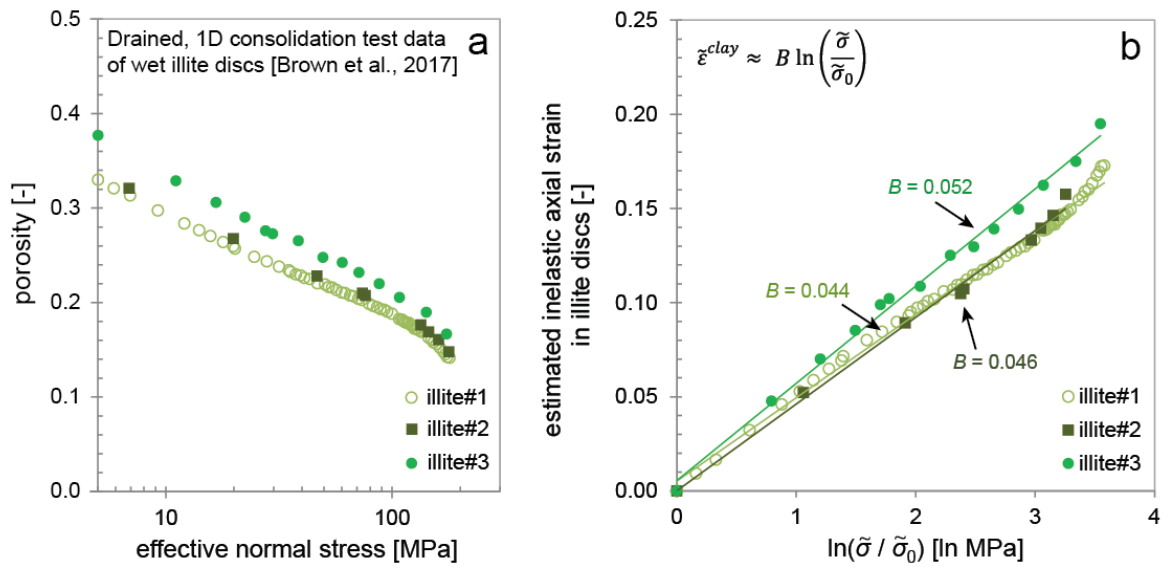


Figure S1a) Plot showing the porosity (ϕ) evolution of wet illite discs (1-2 mL) with increasing effective axial stress (σ), calculated from the void ratio ($= \phi/[1 - \phi]$) versus σ data obtained in the drained, 1-D consolidation tests performed by *Brown et al.*, [2017]; **b)** After subtraction of the expected elastic component (see text), the estimated 1-D, inelastic porosity reduction, or inelastic axial strain of the illite films (in our model denoted: $\tilde{\epsilon}^{clay}$) can be described by a log-linear relation, as shown. In our model, the illite films are present on grain contacts, whereby σ is given by the effective contact normal stress ($\tilde{\sigma}$) and $\tilde{\sigma}_0$ is an initial, reference contact effective normal stress.

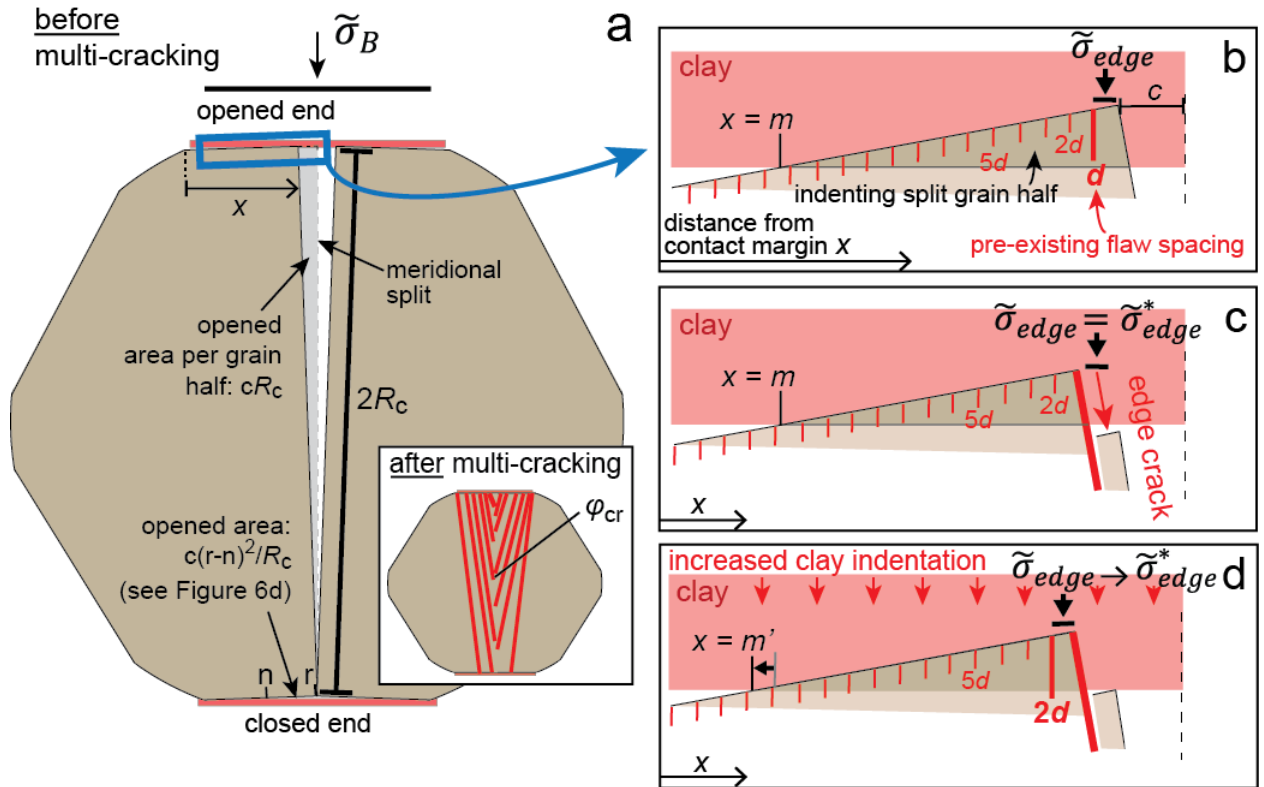


Figure S2: Diagrams illustrating the geometry and geometrical parameters considered in our analysis of intragranular, multi-edge cracking, following initial meridional splitting at assumed constant grain contact stress $\tilde{\sigma}_B$ during deviatoric compression at $\theta = 0^\circ$. **a)** After splitting, the cross-sectional area of the opened gap is the sum of the opened cross-sectional area of the split, plus that at the closed end of the crack, along $n > x \geq r$ (refer Figure 6d). **b)** Detailed view on one side of the split grain contact, at the opened end. Along this contact, pre-existing flaws are assumed present at a regular distance d . The normal stress ($\tilde{\sigma}_{edge}$) acting on the most uplifted edge within one flaw spacing (d) of the initial meridional crack will be strongly enhanced due to clay indentation and will tend to extend the first neighboring contact flaws to produce an edge crack. **c)** When $\tilde{\sigma}_{edge}$ equals the critical value $\tilde{\sigma}_{edge}^*$ for edge crack propagation, two slices alongside the meridional split will break off, be displaced into the gap opened by the split, and cease to support load; **d)** At assumed constant applied stress, the reduction in supported load causes the grain halves to indent further into the clay, leading to again enhanced loading of the next edge, between $(r - 2d) > x \geq (r - d)$, which then instantly reaches $\tilde{\sigma}_{edge}^*$. At constant stress, this unstable sequence of clay-indentation and breaking off slices progresses until the opened gap is filled such that the broken-off slices start to support load.